Preprint for Smart Mater. Struct. 23 (2014) 125021 [doi:10.1088/0964-1726/23/12/125021]

Biaxially crumpled silver thin-film electrodes for dielectric elastomer actuators

Sze-Hsien Low and Gih-Keong Lau

School of Mechanical & Aerospace Engineering, Nanyang Technological University, 50 Nanyang Avenue, Singapore 639798, Singapore.

E-mail address: mgklau@ntu.edu.sg

Metal thin films, which have high-conductivity, are much stiffer and may fracture at a much lower strain than dielectric elastomers. In order to fabricate compliant electrodes for use in dielectric elastomer actuators (DEAs), metal thin films have been formed into either zigzag patterns or corrugations, which favour bending and only allow uniaxial DEA deformations. However, biaxially compliant electrodes are desired in order to maximise generated forces of DEA. In this paper, we present crumpled metal thin-film electrodes that are biaxially compliant and have full area coverage over the dielectric elastomer. These crumpled metal thin-film electrodes are more stretchable than flat metal thin films: they remain conductive beyond 110% radial strain. Also, crumpling reduced the stiffening effect of metal thin films on the soft elastomer. As such, DEAs using crumpled metal thin-film electrodes managed to attain relatively high actuated area strains of up to 128% at 1.8 kV (102 $V\mu m^{-1}$).

1 Introduction

Compliant electrodes are essential for dielectric elastomer actuators (DEAs) to generate large strokes: the electrodes should be electrically conductive and as stretchable as the activated elastomer; equally important is that they have low stiffness, so as to not impede large deformations of the soft elastomer. Compliant electrodes are usually made of conductive particles, in the form of dry powder or suspended in grease. However, particulate and grease electrodes adhere poorly to the elastomer's surface and are hence not stable over repeated actuations. For example, greases may dry up or get rubbed off, while powders may dislodge; this results in a reduction, or even a loss, in electrical conductivity over cycles [1]. These issues of electrode stability can be alleviated by impregnating the conductive particles in the elastomer matrix, so as to prevent their ablation [2-4]. However, such electrodes generally have high electrical resistances, typically above the range of kΩ/□. A lower electrical resistance can be attained by impregnating more conductive particles, but this leads to an increase in electrode stiffness [4]. In order to address these issues of stability and electrical resistance, metal thin-film electrodes can be considered for use in DEAs.

Metal thin films on elastomeric substrates [6-8] have been proven to make reliable stretchable electrodes with low electrical resistances. Although flat metal films fracture easily upon stretching [5], they can readily flex without fracture [9]. They can be designed into a stretchable form that favours

flexing and allows large deformations of elastomeric substrate [10-12]. Serpentine patterning can make metal thin films on elastomers stretchable in the in-plane direction [12-16], but it reduces the electrode area coverage; this would result in a decrease in the generated electrostatic force. Alternatively, the corrugation of metal thin films on elastomer substrates offers full area coverage and uniaxial stretchability [17-23]. For example, Danfoss PolyPower's corrugated silver thin-film electrodes could be mechanically stretched by up to 80% linear strain [24], while its DEAs could actuate up to 15% linear strains [22]. However, corrugated metal thin-film electrodes are generally stiffened in the transverse axial direction [25-27] and are consequently almost inextensible in that direction.

Biaxially compliant electrodes are required to maximise electrostatic force generation in DEAs. With a biaxial area expansion of electrodes, the electrostatic force generated is more than that generated with a constant electrode area [28, 29]. As a result, DEAs using biaxially compliant grease electrodes can exhibit enormous actuation strains. It would be highly desirable if metal thin-film electrodes could be as biaxially compliant as conductive greases, while possessing the added benefits of high conductivity and stability, both electrically and structurally. Biaxial corrugations or wrinkles in metal thin films can be induced via thermal mismatch [30-33]. However, the few reported biaxially stretchable metallic electrodes [12, 34] do not appear to be compliant enough to allow large bi-axial deformation of DEAs. In this paper, we present biaxially compliant metal thin-film electrodes, which were mechanically buckled on the dielectric elastomeric substrate and can electrically unfold. Subsequent sections will present the working principles, analysis, fabrication, and characterisation of these electrodes and their use in DEAs.

2 Biaxially crumpled metal thin films as compliant electrodes

In this study, we develop biaxially compliant DEA electrodes comprising crumpled metal thin films on elastomer substrates. The metal thin films on the surfaces of the elastomer substrate were buckled by mechanically-induced biaxial compressive strains. When stretched, the crumpled metal thin films readily unfold. Due to this propensity to bend, crumpled thin films appear to be axially less stiff than flat thin films. As such, crumpled metal thin films can be used as biaxially compliant electrodes for DEA deformations. This is as opposed to corrugated metal thin films that are only uniaxially compliant.

Figure 1 shows how crumpled metal thin-film electrodes are prepared. First a stress-free elastomer of diameter D_0 is highly stretched to a diameter of D_l. Following that, a pair of metal thin films is electrolessly plated on either side of the highly-stretched elastomer. In this state, the elastomer is

highly-stretched while the metal thin films are relatively stress-free and flat. By reducing the stretch in the elastomer, from a diameter of D_I to D_{II}, induced biaxial compressive strains cause the metallic surfaces of the elastomer to buckle, thereby forming crumpled metal thin-film electrodes.

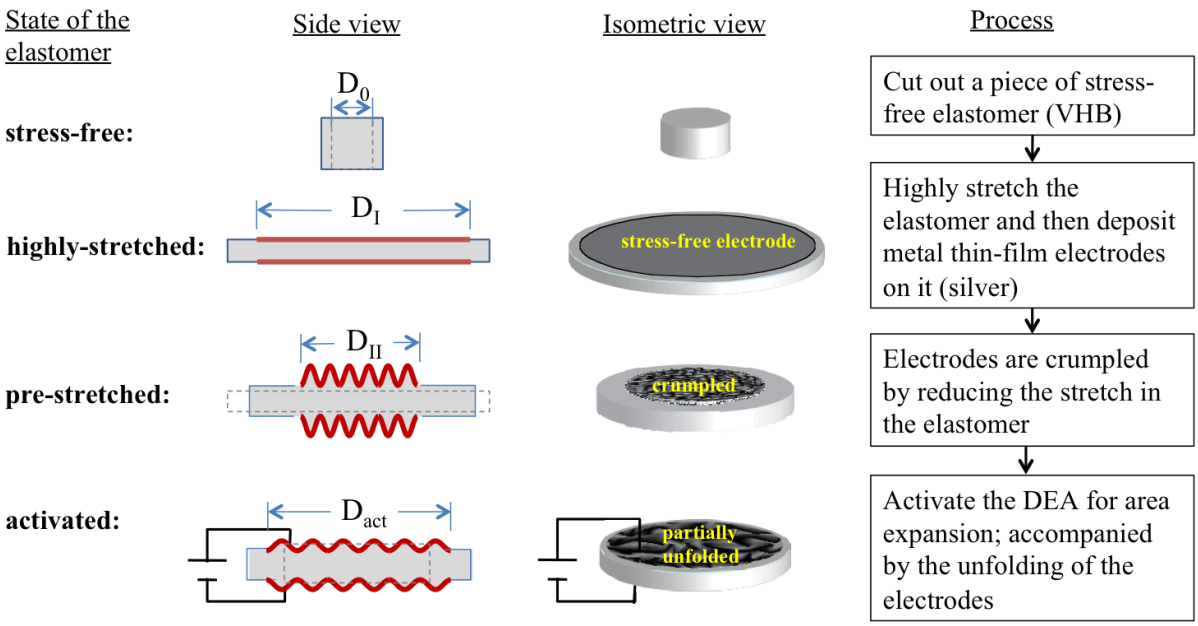

Figure 1. Schematic illustrating the fabrication and activation of a membrane DEAs with crumpled metal thin-film electrodes.

In this pre-stretched state, the elastomer substrate is under tension and has a radial pre-stretch ratio of

$$\lambda_p = \frac{D_{II}}{D_0} \quad (1)$$

while the buckled metal thin films are subjected to an apparent compressive strain of

$$c = \frac{D_I - D_{II}}{D_I} = 1 - \frac{D_{II}}{D_I} \quad (2)$$

Upon activation by Maxwell stress, the membrane DEA expands in area to an activated diameter of D_{act}. The electrically-induced area strain is given by:

$$s_A = \left[\left(\frac{D_{act}}{D_{II}}\right)^2 - 1\right] \% \quad (3)$$

This area expansion is accompanied by the unfolding and the flattening of the crumpled metal thin-film electrodes.

3 Stiffness analysis for buckled metal thin films

Compliant electrodes should conform to its elastomer substrate and not impede large deformations. To do so, the electrodes should have a low stiffness in the plane of area expansion. It is difficult to stretch a metal thin film but relatively easy to flex it. As such, uniaxial or biaxial buckling could significantly reduce the apparent axial stiffness of metal thin films. Although difficult to measure experimentally, the apparent stiffness of thin films can be theoretically estimated using structural plate analysis [25].

3.1 Uniaxial buckling with a harmonic profile

The apparent axial modulus of a corrugated thin film can be estimated by considering a representative strip of metal thin film, which is subjected to one pair of compressive forces per unit length, N_x. The lateral (z-direction) displacement w of the buckled thin film is assumed to have a sinusoidal profile [25]:

$$w = \zeta \sin(\frac{\pi x}{l}) \tag{4}$$

in which ζ is the amplitude of the corrugation and l is the half-wavelength of the corrugation, along the x axis, as shown in figure 2b.

Using a small-displacement approximation, the arc length l_0 of the buckled thin film is

$$l_0 = \int_0^l \sqrt{1 + \left(\frac{dw}{dx}\right)^2}\, dx \approx \left(1 + \frac{\pi^2 \zeta^2}{4l^2}\right) l \tag{5}$$

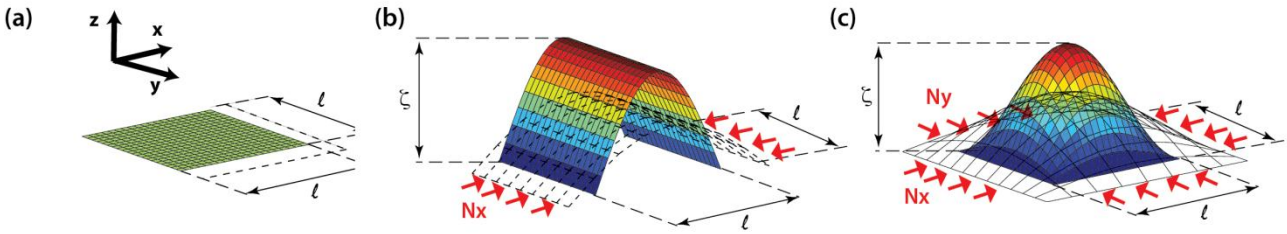

Figure 2. Dimensions and deformations of a (a) flat (b) uniaxially buckled and (c) biaxially buckled thin film.

Assuming that there is negligible axial strain in the middle plane of the thin film, the buckled thin film bends from its original length of l_o to get packed into a shorter half-wavelength l. Hence, the apparent axial strain is defined as the ratio of half-wavelength reduction over the arc length:

$$c_x = \frac{l_o - l}{l_o} = \frac{\pi^2 \zeta^2}{4l^2 + \pi^2 \zeta^2} \quad (6)$$

Using the principle of virtual work, the compressive force per unit length is derived as (see appendix A1)

$$N_x = \frac{Eh^3}{12(1-\upsilon^2)}\left(\frac{\pi^2}{l^2}\right) \quad (7)$$

wherein h is the film thickness, while E and υ are the Young's modulus and Poisson's ratio of the metal thin film, respectively.

Assuming elastic deformation, the compressive forces required to buckle the thin film is equal to the tensile forces required to flatten it. The apparent Young's modulus is therefore the ratio of the compressive axial stress over the apparent strain:

$$E_{x,uniaxial} = \frac{N_x}{hc_x} = \left(\frac{\pi^2}{12(1-\upsilon^2)}\right)\left(\frac{h}{l}\right)^2\left(\frac{1}{c_x}\right)E \quad (8)$$

Using equation (8) and noting that the thin-film's thickness is typically in the nano-scale while the wavelength is in the micro-scale [17, 23], it can be seen in figure 3 that the apparent axial Young's modulus of a uniaxially buckled thin film is lower than that of a flat thin film.

Although uniaxial buckling is able to make thin films more compliant in one direction (along the x-axis), it stiffens the thin film in the transverse direction (along the y-axis). In fact, in large structures, corrugated plates are often used for their enhanced stiffness along the y-axis. With an increased cross-sectional area over the same half-wavelength, the uniaxially buckled thin film has a transverse apparent Young's modulus of

$$E_{y,uniaxial} = \left(\frac{1}{1-c_x}\right)E \quad (9)$$

which is greater than that for the flat thin film as $1\text{-}c_x$ is less than one.

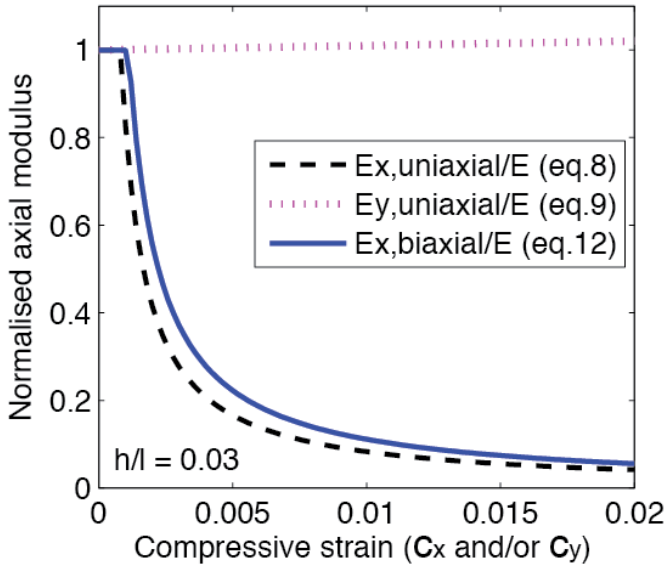

Figure 3. Change in the apparent axial modulus of the thin film (normalised by the Young's modulus of the material) due to uniaxial and biaxial compressions for a given half-wavelength.

3.2 **Biaxial buckling with a bi-harmonic profile**

Unlike uniaxially buckling, which makes a metal thin film more compliant in one direction but stiffer in the other, biaxial buckling makes a metal thin film equally compliant in both the axial and transverse directions.

The apparent axial modulus of a biaxially crumpled metal thin film can be estimated by considering a representative square strip of metal thin film, which is compressed biaxially by two orthogonal pairs of equal forces per unit length, i.e. N_x, $=N_y$. The lateral (z-direction) displacement w of this biaxially buckled thin film is assumed to have a bi-harmonic profile [25] (see figure 2c):

$$w = \zeta \sin(\frac{\pi x}{l}) \sin(\frac{\pi y}{l}) \qquad (10)$$

wherein l is the identical half-wavelengths along the orthogonal axes of x and y.

Using the principle of virtual work and assuming small deformations [35], the equal biaxial compressive force per unit length is (see appendix A2)

$$N_x = \frac{Eh^3}{6(1-v^2)}\left(\frac{\pi^2}{l^2}\right) \quad (11)$$

Again, assuming elastic deformation, the compressive forces required to buckle the thin film is equal to the tensile forces required to flatten it. Hence, the apparent axial modulus in the *x* axis can be calculated as the ratio of the apparent axial stress to the apparent strain, following [25]:

$$E_{x,biaxial} = \frac{N_x - vN_y}{hc_x} = \left(\frac{\pi^2}{6(1+v)}\right)\left(\frac{h}{l}\right)^2\left(\frac{1}{c_x}\right)E \quad (12)$$

Due to symmetry and equal biaxial loading, the axial moduli along the two orthogonal directions are equal, such that

$$E_{y,biaxial} = \frac{N_y - vN_x}{hc_y} = E_{x,biaxial} \quad (13)$$

As seen in figure 3, like uniaxially buckled thin films, the axial apparent Young's modulus of a biaxially buckled thin film is also lower than the Young's modulus of a flat thin film. However, when the thin film is biaxially buckled, its stiffness is reduced in both the axial and transverse directions; this is in contrast to uniaxially buckled thin films, wherein stiffness is increased in the transverse direction. As such, biaxially buckled metal thin films are suitable for use as biaxially compliant electrodes for DEAs.

4 Fabrication

In the typical fabrication of membrane DEAs, the elastomer was stretched to a pre-stretch ratio of λ_p (see equation 1) and then coated with electrodes. However, to fabricate crumpled (buckled) metal thin-film electrodes, see figure 1, the elastomer had to first be highly-stretched, to a stretch ratio higher than λ_p. In this highly-stretched state, stress-free metal thin films were deposited on the elastomer. Subsequently, as the stretch in the elastomer was reduced to λ_p, the induced compressive strain *c* (see equation 2) in the metal thin films caused them to crumple. In order to vary the amount of compressive strain in the crumpled electrodes, while maintaining the same pre-stretch, the stretch at which the electrodes were deposited was altered. For example, to attain a DEA with $\lambda_p = 2.5$ and $c = 0.4$, metal thin films have to be deposited on an elastomer that had been highly-stretched by 4.2 times.

The stretching and relaxation of the elastomer (VHB F9473PC, 3M) was carried out via a custom-made radial stretching jig, as shown in the appendix, at a rate of 0.06 D_0 per second.

In this work, a 250μm thick VHB9473PC tape is used as the dielectric elastomer instead of the more commonly adopted 1mm thick VHB4910 because the thinner tape can reduce the pre-load required to achieve the same pre-stretch. In addition, according to the 3M data sheet, the thinner tape of VHB9473PC in its non-stretched form is reported of a higher dielectric strength at 5500V/mil [36], which is higher than 630V/mil [37] of the thicker VHB4910 tape in the non-stretched form. Previously, the non-stretched form of silvered VHB9473PC tape was used to make multi-layered dielectric elastomeric unimorph [38], capable of a large bending; whereas, the bi-axially pre-stretched form of the silvered tape demonstrated up to 50% areal strain at high breakdown field of 350MV/m [39].

The morphology of the buckled metal thin film depends on the amount of compressive strain that it had been subjected to (Figure 4). Initially, the stress-free metal thin film was rather flat, conforming to the surface morphology of the pre-stretched VHB membrane. When the metal thin film was subjected to 20% compressive strain, deep folds and fine fault lines formed, dividing the continuous metallic thin film into fragments. As the amount of compressive strain increased further, the thin-film fragments buckled further, changing from mild wrinkles to deep folds. At 50% compressive strain, fine twisted folds formed on the existing wrinkle, giving a nested hierarchy [40]. Under large biaxial compressions, a metal thin film transforms into a complex combination of deep folds and tightly-packed wrinkles. As such, we have coined these electrodes as crumpled metal thin-film electrodes.

The metal thin films in the crumpled electrodes were electrolessly plated on the elastomer substrate. The electroless deposition (ELD) method is commonly used to metalize a glass substrate to form a mirror-like surface under normal room conditions; it does not require a vacuum, unlike the sputtering deposition method. Previously, our group found that DEAs with ELD silver electrodes can actuate better than DEAs with sputtered silver electrodes [39]. A three-part silvering solution set (HE-300, Peacock Laboratories, Inc.) that comprised a silver diammine complex, a sodium hydroxide activator and a reducing agent was used. Each solution-part was first diluted with forty parts of deionized water. The elastomer area, which was to be plated, was sensitised by using a tin catalyst (1 part No. 93 Sensitizer to 30 parts deionized water) while the non-electrode area was masked by a silicone stencil. Following that, a fresh mixture of the three-part diluted silvering solutions was dripped onto the wetted area. As the chemical reaction completes, the sensitized area was coated with a thin film of silver. Typically, a 1 minute reaction time yields a silver thin film of 150 ± 30 nm thick; the thin-film thickness was obtained by using an atomic force microscope to measure the step-height of ELD silver thin films that had been deposited on a glass slides. The thickness variation was due to the manual dispense of chemicals and a non-uniform deposition rate.

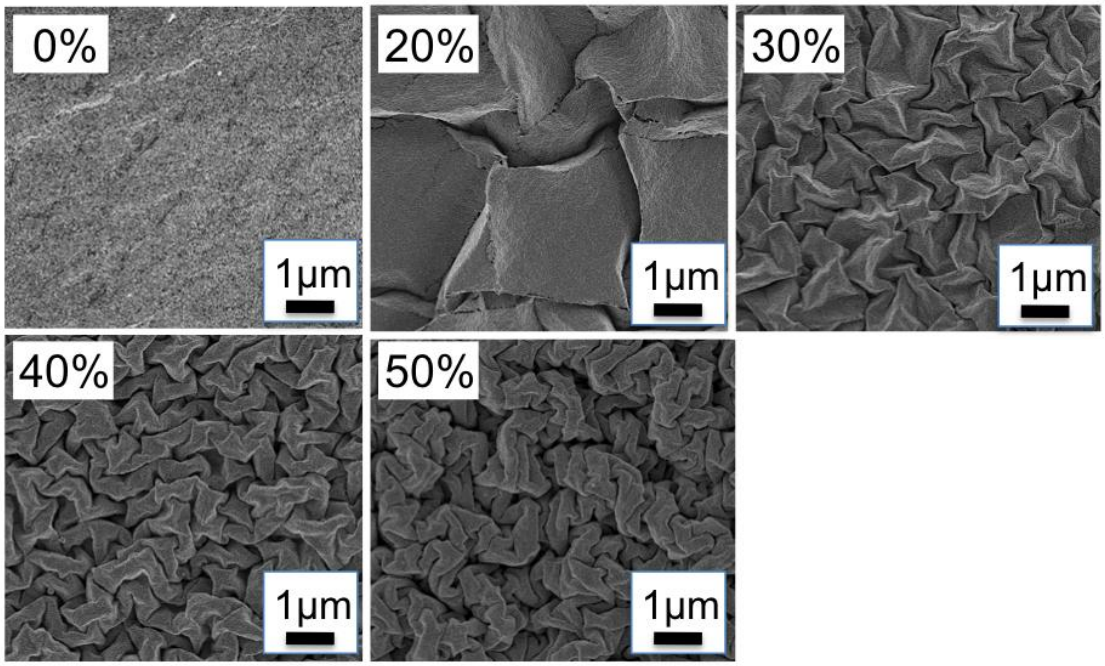

Figure 4. Change in morphology as the silver thin film was subjected to varying amounts of compressive strain.

5 Properties of crumpled metallic thin film

Applying a pair of electrodes onto an elastomer membrane stiffens it. To measure this stiffening effect, electrode-elastomer membrane composites were radially stressed, starting from an initial equi-biaxial pre-stretch of 2.5. A setup similar to the radial stretching jig shown in appendix B was used, except that the motor was replaced by an eight-pulley system. Radial forces of equal magnitude F were applied at the eight equally spaced points on the circumference of the electrode-elastomer membrane. Those radial forces were imposed by adding dead-weights at a rate of 2.6 grams per minute. The radial stress σ_R in the electrode-elastomer membrane, over the circumference of a circular disk of diameter D and initial diameter D_0, is calculated to be

$$\sigma_R = \frac{\sum F}{\pi D t} \qquad (14)$$

where t is the electrode-elastomer membrane thickness. With increasing stretch ratio $= D/D_o$, the radial stress σ_R increases, as shown in figure 5. The gradient of the electrode-elastomer membrane's stress-stretch ratio provides a measure for the radial modulus E_R of the electrode-elastomer membrane

$$E_R = \frac{\Delta\sigma_R}{\Delta\lambda} \quad (15)$$

in which $\Delta\sigma_R$ is the radial stress increment over the stretch-ratio increment $\Delta\lambda$.

The type of electrode material was found to influence the apparent radial stiffness to different extents. As graphite powder and silver thin films have been used as solid-state electrodes for DEAs, they have been chosen to serve as performance comparisons for the crumpled silver thin films. Doing so should help illustrate the electrodes' stiffening effect on the soft dielectric elastomer, as well as its impact on the actuations of DEAs. Three types of reference electrode materials were tested: sputtered silver thin film (150nm thick), ELD silver thin film (150nm ± 30nm thick) and graphite powder (10μm thick). The sputtered silver thin film was prepared by means of a magnetron sputtering process; the graphite coating was prepared by sprinkling a small amount of graphite powder on the elastomer and then gently tapping it in with a paintbrush. The thickness of the metal thin films were obtained by using an atomic force microscope to measure the step-height of the thin films that had been deposited on glass slides, while the thickness of the graphite powder coating was measured from its topography using a confocal microscope. These three electrode materials were coated onto equi-biaxially pre-stretched (λ_p=2.5) elastomer membranes (VHB F9473PC) to form relatively stress-free 40mm diameter electrodes. On the other hand, 40% crumpled electrodes of the same diameter were prepared by relaxing a 4.2 times stretched elastomer membrane, with ELD silver thin films on it, to a 2.5 times pre-stretch. For each type of electrode, at least three samples were prepared and tested.

The electrode's stiffening effect was observed when the radial moduli of electrode-clad elastomer membranes were compared with the modulus of the plain membrane. As a reference, the plain pre-stretched VHB membrane was found to have a radial modulus of 402 kPa. Flat silver thin films have been found to greatly stiffen the elastomer membrane: the sputtered-silvered membrane being 3 times stiffer than the plain membrane and the ELD silvered membrane being 2.6 times stiffer. The graphite powder coating was found to minimally stiffen the elastomer membrane by 8%. Interestingly, the crumpled silver thin films also showed little stiffening effect; the elastomer membrane with crumpled electrodes was 13% stiffer than the plain elastomer membrane. Unlike other electrodes, the crumpled metal electrodes add a residual stress to the elastomeric membrane, requiring a higher membrane pre-stress at the same membrane stretch.

DEAs remain functional, even when using high-resistance compliant electrodes [19]. In view of this, the stretchability of a compliant electrode is defined as the maximum stretch at which it has an electrical resistance of less than 1 GΩ, which is near to the resistance measurement limit of the digital multimeter used (Agilent 34410A). Several electrode materials were tested for their stretchability:

graphite powder, plain sputtered silver thin film, plain ELD silver thin film and 40% crumpled ELD silver thin film. These electrode materials were coated to form 50 mm diameter circular electrodes on elastomer membranes with the same amount of pre-stretch. During the test, each electrode-elastomer membrane was stretched incrementally at a rate of 34% radial strain per minute. The resistance across the electrode diameter was measured simultaneously, by means of a four-wire connection, using the multimeter. For each electrode material, at least three samples were prepared and tested.

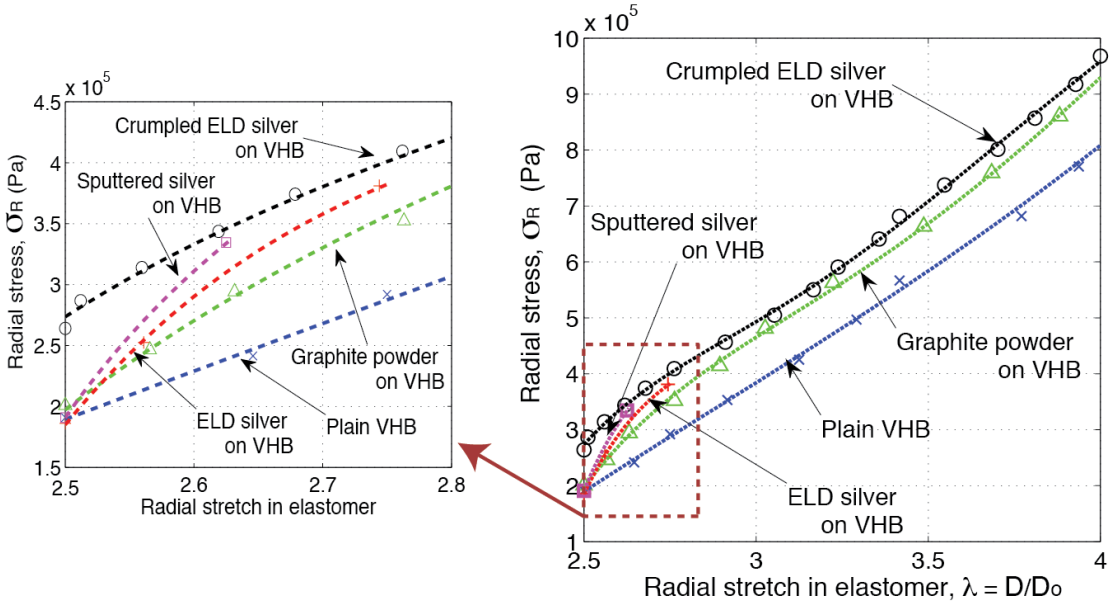

Figure 5. Stiffening effect of different types of electrodes on the electrode-elastomer membrane composites subject to radial stretches.

Figure 6 shows that the measured resistance increases at an increasing rate with respect to radial stretch. As the radial stretchability of a circular electrode is influenced by its shape, each electrode's resistance change, instead of resistivity, was plotted with respect to the radial stretch in the elastomer. ELD silver thin films, with the lowest initial resistance of 10 Ω, could only be stretched up to 10% radial strain, beyond which it cracked into fine isolated grains and lost its electrical continuity [39]. Graphite powder electrodes, which had a higher initial resistance of 51kΩ, could be stretched up to 50% radial strain, beyond which the network of conductive particles disconnected. Interestingly, the 40% crumpled silver thin film could be stretched up to 110% radial strain, before reaching a resistance of 1GΩ. This 11-fold improvement over the plain ELD silver thin film can be attributed to the unfolding capability of the crumpled form, which helps delay the widespread crack formation in the metal thin film under high tension. However, the 40% crumpled electrode had a higher initial resistance, of 90 Ω, as compared to that of the plain, flat metal electrode. This was because initial micro-cracks had formed in the crumpled silver thin films during the fabrication process, thereby causing an increased electrical resistance. These micro-cracks did not propagate under cyclic uniaxial

loading as the resistance change with stretch remained stable throughout the hundred cycles (see appendix C).

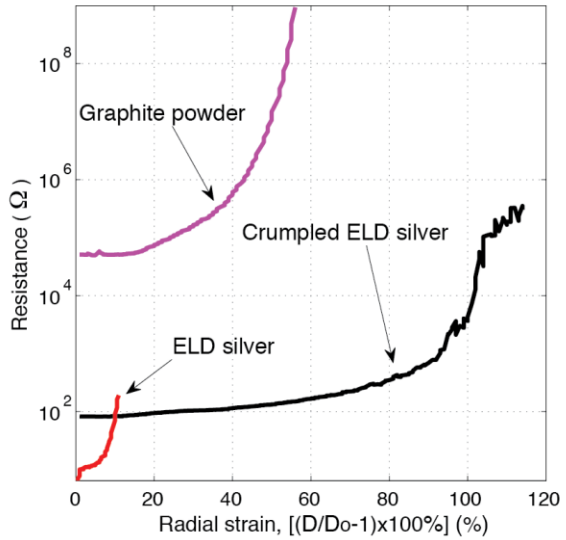

Figure 6. Radial stretchability of different types of electrodes.

6 Electromechanical Actuation

Crumpled metal thin-film electrodes can be used as compliant electrodes for DEAs that require biaxial deformations as they have been found to be highly stretchable and only slightly stiffens its elastomer substrate (see section 5). Here, membrane DEAs using 40% crumpled ELD silver thin-film electrodes were prepared as described before: a 4.2 times stretched elastomer membrane, on which initially stress-free ELD silver thin films were deposited, was relaxed to a 2.5 times pre-stretch. However, due to the stiffness of the electrode trails, the initially circular stress-free silver electrodes crumpled into an oval shape of approximately 10mm in diameter. This pre-stretched membrane DEA was subsequently transferred to a 50 mm square acrylic frame for support.

Activation of the DEAs, using a high voltage source (Trek 610E), caused the electrodes to expand with a large area strain. As shown in figure 7, the actuated area strain was 103% at 1.6 kV ($80 V\mu m^{-1}$) and further increased to 128% at 1.8 kV ($102\ V\mu m^{-1}$). During the area expansion, the crumpled electrodes were observed to unfold from the fine wrinkles into the coarse ones (see figure 8). Such large actuation strains, of DEAs using crumpled silver thin-film electrodes, are comparable to the actuation strains produced by DEAs using graphite powder electrodes, as shown in figure 9, and is a marked improvement over the actuation capability of DEAs using plain silver thin-film electrodes.

This can be attributed to the reduction of the silver thin films' apparent Young's modulus due to crumpling.

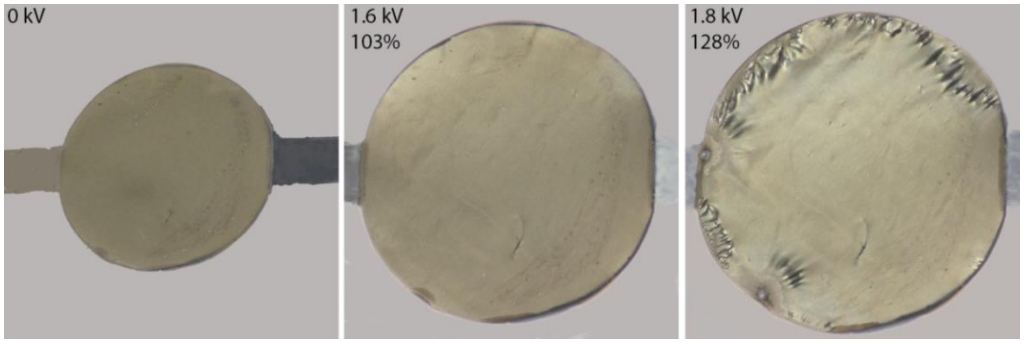

Figure 7. Photographs showing the top view of a 2.5 times biaxially pre-stretched membrane DEA with crumpled ELD silver electrodes under an initial compressive strain of 40%.

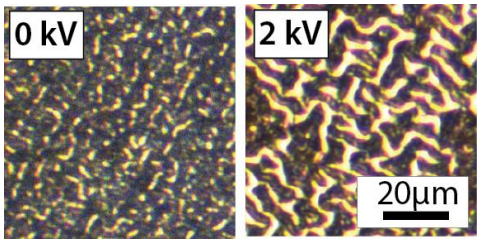

Figure 8. The micrographs (taken from a different sample as in figure 7) illustrate the unravelling of the folds during activation at 2kV. The corresponding actuated area strain is approximately 90%.

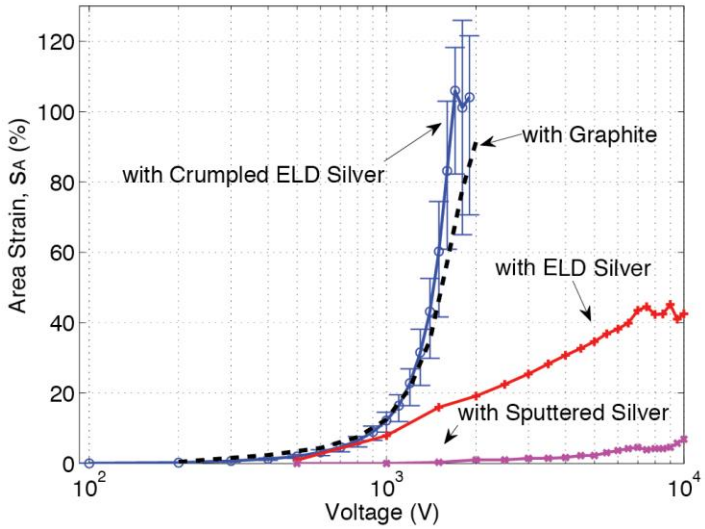

Figure 9. Actuated area strain as a function of driving voltage for DEAs using different electrode materials. Ten samples for the crumpled ELD silver DEAs were tested and error bars indicate the standard deviation.

So far, it has been shown that crumpling ELD silver thin films by 40% results in a lower apparent Young's modulus; it would be interesting to find out if the extent of crumpling affects its apparent Young's modulus, such that it manifests in the actuated strains of DEAs. As described in section 4, on the fabrication of crumpled silver thin films, the greater the extent of electrode compression, the more and deeper the folds. This in turn affects its apparent Young's modulus, according to equation (8), thereby influencing the achievable electromechanical actuation of the DEA. As shown in figure 10, the maximum actuated strain achievable by DEAs varied with the extent of electrode crumpling, even though they all had the same elastomer pre-stretch. That is to say, for a 40% crumpling, silver thin films are deposited on a 4.2 times stretched elastomer, before the stretch is reduced to a 2.5 times pre-stretch; as for a 10% crumpling, silver thin films are deposited on a 2.8 times stretched elastomer, before the stretch is reduced to 2.5 times pre-stretch. DEAs with plain metal thin-film electrodes produced the least actuation due to the large stiffening effect of its electrodes. As shown in figure 11, DEAs with crumpled metal thin-film electrodes generally fared better with more electrode crumpling, up to 40% compressive strain. However, too much crumpling made the electrodes stiffer. This was caused by a reduction in the wavelength and an increase in the effective thickness of the electrodes, due to a nested hierarchy of wrinkles and folds (refer to equation (8)). Consequently, DEAs using 50% electrode crumpling actuated less than that with 30% electrode crumpling.

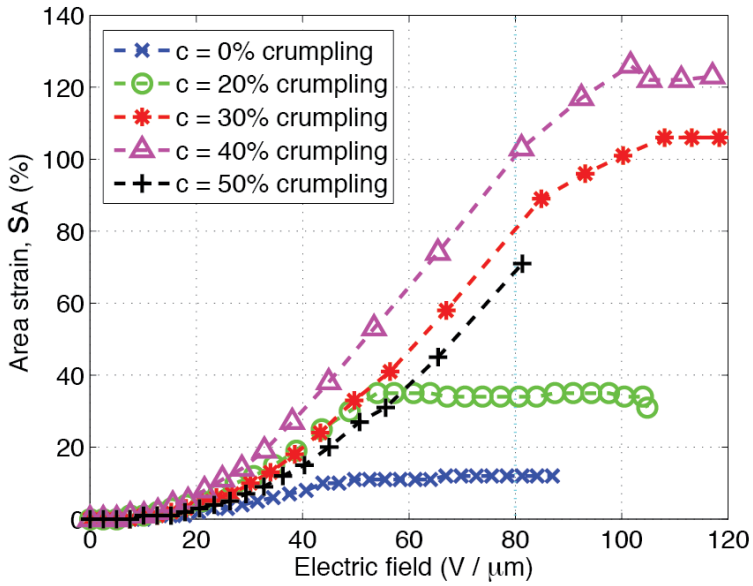

Figure 10. Actuated area strain, with respect to the applied electric field, of DEAs using ELD silver thin-film electrodes that had been crumpled by 0%, 20%, 30%, 40% and 50% compressive strains.

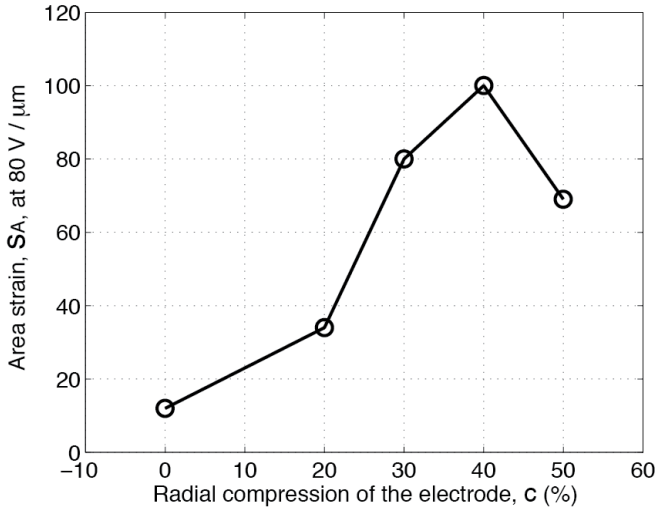

Figure 11. Actuated area strain (at an electric field of 80 Vμm^{-1}) obtained by membrane DEAs with ELD silver electrodes that were crumpled to varying degrees.

7 Self-Clearing

Silver thin-film electrodes have been reported to be able to self-clear [22, 39], which can help to stop localized electrical breakdown from prematurely damaging DEAs. In this case, the crumpled silver thin-film electrodes were also found to be able to self-clear on DEAs. Typically, a DEA has an electrical breakdown localized at a defective spot. For example, the sample shown in figure 12 was subjected to a localized breakdown, wherein purplish sparks were observed at the defective spot near the electrode edge. During the breakdown, the leakage current surged and the driving voltage fell as shown in figure 13. The electrical shorting caused the area strain of the DEA to decrease to 31%, lesser than the achievable strain at the pre-set voltage of 2kV. The elastomer membrane was punctured, as shown in figure 14a, due to the high current flow and joule heating at the shorting spot. The electrical breakdown oxidized the silver thin film surrounding the defective spot and eventually isolated the spot, thereby stopping the breakdown. As the localized defect has been self-cleared, the current leakage was stopped and the pre-set driving voltage restored. Consequently, this self-cleared DEA sample actuated area strain increased to 84% at 2kV, as shown in figure 12.

Self-clearing can occur multiple times in a single DEA prior to total failure. As shown in figure 13, upon increasing the driving voltage by another 100V, a second localised breakdown occurs, which then self-clears again to enable an elevated driving voltage of 2.1kV. This sequence takes place once more before the DEA fails at an applied voltage of 2.2kV. Although self-clearing electrodes allow higher driving voltages, they should only be used for preventing localised breakdowns at a few spots.

This is because self-clearing results in the passivation of the surrounding electrode material, which makes those regions non-conducting, thereby compromise the actuated strains. Ill-positioned self-cleared sites in the middle of a DEA, as shown in figure 14, result in the formation of large wrinkles, which also reduces in-plane actuated strains. As such, while self-clearing electrodes cannot compensate badly manufactured DEAs that are full of flaws, they are very useful for preventing the premature breakdown of DEAs that have just a few localised defects.

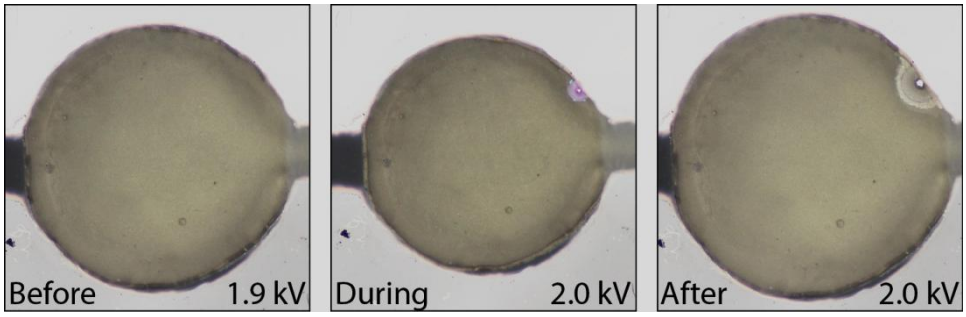

Figure 12. Photographs of the top view of a DEA with crumpled ELD electrodes that undergo self-clearing. Before the event, at 1.9 kV, the area strain was 63%. After the driving voltage was increased to 2 kV, an electrical breakdown occurred, causing the area strain to decrease to 31%. However, after the self-clearing event, at the same driving voltage of 2 kV, the area strain increased to 84%.

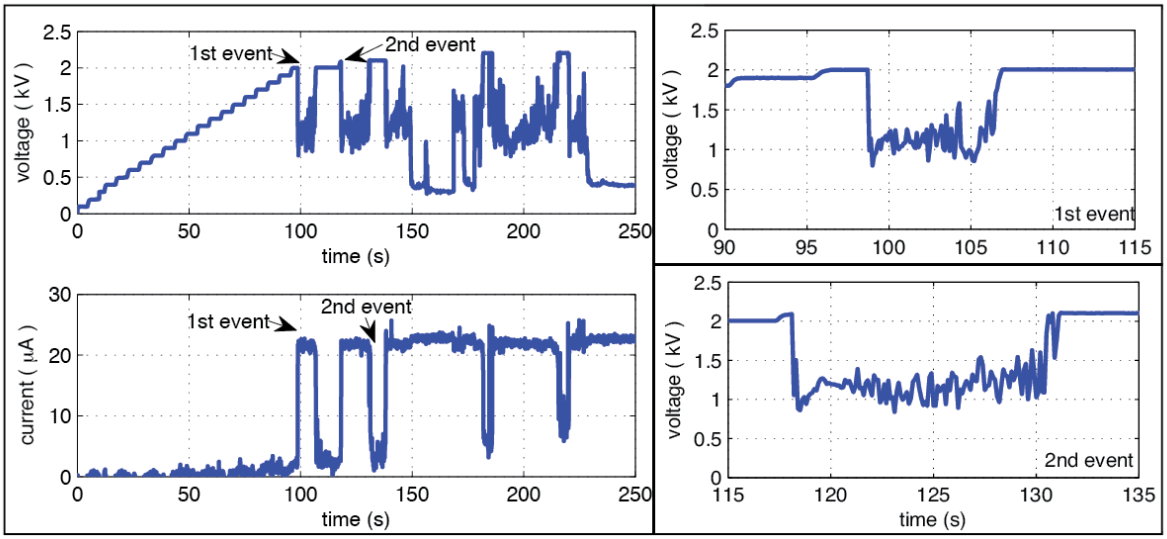

Figure 13. Time histories of voltage and current show an electrical breakdown that is followed by self-clearing, as indicated by a spike in current and a corresponding plunge and recovery in voltage. Four self-clearing event are shown, of which the voltage change during the 1st and 2nd events are magnified.

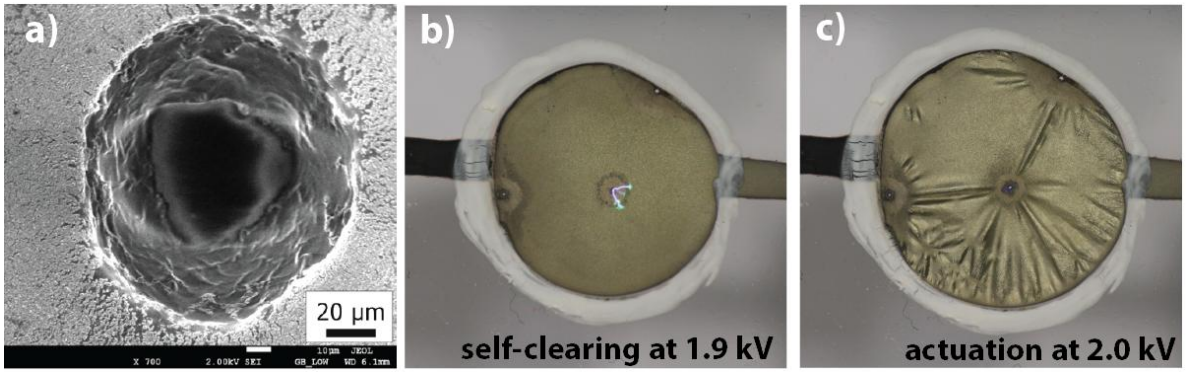

Figure 14. a) a self-cleared site in a DEA membrane sample with crumpled ELD silver thin-film electrodes. b) arc discharge at self-clear site in the middle of the actuator. c) wrinkling of the actuator due to passivated self-clear sites. (the white borders around the electrodes in (b) and (c) is ink used for imaging purposes)

8 Conclusions

Crumpled ELD silver thin films have great potential for use as compliant electrodes for dielectric elastomer transducers. These metallic compliant electrodes are radially stretchable to more than 110% strain. More notably, the stiffening effect on soft elastomers, by these crumpled metal thin films, is much lower than that by flat metal thin films. As such, DEAs using crumpled silver thin-film electrodes can achieve much higher actuated area strains, of more than 120%, than DEAs using flat metal thin-film electrodes. Furthermore, like metal thin-film electrodes, these crumpled electrodes also have the ability to self-clear, which can help to improve the reliability of the DEA. Crumpled ELD silver thin-film electrodes are promising for use in larger-scale dielectric elastomer generators (DEGs) due to its relatively low resistance, which can help to reduce parasitic resistive losses [41], as compared to carbon-based electrodes. Subsequent work will investigate the feasibility of using such electrodes in DEGs.

References

[1] Rosset S and Shea H 2013 Flexible and stretchable electrodes for dielectric elastomer actuators *Appl. Phys. A* **110** 281-307

[2] Hyun D C, Park M, Park C, Kim B, Xia Y, Hur J H, Kim J M, Park J J and Jeong U 2011 Ordered zigzag stripes of polymer gel/metal nanoparticle composites for highly stretchable conductive electrodes *Advanced Materials* **23** 2946-50

[3] Urdaneta M G, Delille R and Smela E 2007 Stretchable Electrodes with High Conductivity and Photo-Patternability *Advanced Materials* **19** 2629-33

[4] Rosset S, Niklaus M, Dubois P and Shea H R 2009 Metal ion implantation for the fabrication of stretchable electrodes on elastomers *Advanced Functional Materials* **19** 470-8

[5] Huang H and Spaepen F 2000 Tensile testing of free-standing Cu, Ag and Al thin films and Ag/Cu multilayers *Acta Materialia* **48** 3261-9
[6] Graz I M, Cotton D P J and Lacour S P 2009 Extended cyclic uniaxial loading of stretchable gold thin films on elastomeric substrates *Applied Physics Letters* **94** -
[7] Lacour S P, Chan D, Wagner S, Li T and Suo Z 2006 Mechanisms of reversible stretchability of thin metal films on elastomeric substrates *Applied Physics Letters* **88** 204103-3
[8] Lacour S, Joyelle P J, Sigurd W, Teng L and Z. S 2006 Elastomeric interconnects *International Journal of High Speed Electronics & Systems* **16** 397-407
[9] Witten T A 2007 Stress focusing in elastic sheets *Reviews of Modern Physics* **79** 643-75
[10] Galler N, Ditlbacher H, Steinberger B, Hohenau A, Dansachmuller M, Camacho-Gonzales F, Bauer S, Krenn J R, Leitner A and Aussenegg F R 2006 Electrically actuated elastomers for electro-optical modulators *Applied Physics B (Lasers and Optics)* **B85** 7-10
[11] Pelrine R, Kornbluh R, Joseph J, Heydt R, Pei Q and Chiba S 2000 High-field deformation of elastomeric dielectrics for actuators *Materials Science and Engineering: C* **11** 89-100
[12] Pimpin A, Suzuki Y and Kasagi N 2007 Microelectrostrictive Actuator With Large Out-of-Plane Deformation for Flow-Control Application *Microelectromechanical Systems, Journal of* **16** 753-64
[13] Gray D S, Tien J and Chen C S 2004 High-Conductivity Elastomeric Electronics *Advanced Materials* **16** 393-7
[14] Hu X, Krull P, de Graff B, Dowling K, Rogers J A and Arora W J 2011 Stretchable Inorganic-Semiconductor Electronic Systems *Advanced Materials* **23** 2933-6
[15] Brosteaux D, Fabrice A, Gonzalez M and Vanfleteren J 2007 Design and Fabrication of Elastic Interconnections for Stretchable Electronic Circuits *Electron Device Letters, IEEE* **28** 552-4
[16] Gonzalez M, Axisa F, Bulcke M V, Brosteaux D, Vandevelde B and Vanfleteren J 2008 Design of metal interconnects for stretchable electronic circuits *Microelectronics Reliability* **48** 825-32
[17] Kim D-H and Rogers J A 2008 Stretchable Electronics: Materials Strategies and Devices *Advanced Materials* **20** 4887-92
[18] Lacour S P, Jones J, Wagner S, Li T and Suo Z 2005 Stretchable Interconnects for Elastic Electronic Surfaces *Proceedings of the IEEE* **93** 1459-67
[19] Rogers J A, Someya T and Huang Y 2010 Materials and mechanics for stretchable electronics *Science* **327** 1603-7
[20] Wang X, Hu H, Shen Y, Zhou X and Zheng Z 2011 Stretchable Conductors with Ultrahigh Tensile Strain and Stable Metallic Conductance Enabled by Prestrained Polyelectrolyte Nanoplatforms *Advanced Materials* **23** 3090-4
[21] Watanabe M, Shirai H and Hirai T 2002 Wrinkled polypyrrole electrode for electroactive polymer actuators *Journal of Applied Physics* **92** 4631-7
[22] Benslimane M Y, Kiil H E and Tryson M J 2010 Dielectric electro active polymer push actuators: performance and challenges *Polymer International* **59** 415-21
[23] Sun Y, Choi W M, Jiang H, Huang Y Y and Rogers J A 2006 Controlled buckling of semiconductor nanoribbons for stretchable electronics *Nat Nano* **1** 201-7
[24] Benslimane M, Kiil H-E and Tryson M J 2010 Electromechanical properties of novel large strain PolyPower film and laminate components for DEAP actuator and sensor applications. pp 764231--11
[25] Timoshenko S and Woinowsky-Krieger S 1959 *Theory of plates and shells* vol 2: McGraw-hill New York)
[26] Lacour S P, Jones J, Suo Z and Wagner S 2004 Design and performance of thin metal film interconnects for skin-like electronic circuits *Electron Device Letters, IEEE* **25** 179-81
[27] Volynskii A L, Bazhenov S, Lebedeva O V and Bakeev N F 2000 Mechanical buckling instability of thin coatings deposited on soft polymer substrates *Journal of Materials Science* **35** 547-54
[28] Pelrine R E, Kornbluh R D and Joseph J P 1998 Electrostriction of polymer dielectrics with compliant electrodes as a means of actuation *Sensors and Actuators A: Physical* **64** 77-85

[29] Sommer-Larsen P, Kofod G, Shridhar M H, Benslimane M and Gravesen P 2002 Performance of dielectric elastomer actuators and materials. In: *Smart Structures and Materials 2002. Electroactive Polymer Actuators and Devices (EAPAD), 18-21 March 2002,* (USA: SPIE-Int. Soc. Opt. Eng) pp 158-66
[30] Huck W T S, Bowden N, Onck P, Pardoen T, Hutchinson J W and Whitesides G M 2000 Ordering of Spontaneously Formed Buckles on Planar Surfaces *Langmuir* **16** 3497-501
[31] Yoo P J, Park S Y, Kwon S J, Suh K Y and Lee H H 2003 Microshaping metal surfaces by wave-directed self-organization *Applied Physics Letters* **83** 4444-6
[32] Yoo P J, Suh K Y, Park S Y and Lee H H 2002 Physical self-assembly of microstructures by anisotropic buckling *Advanced Materials* **14** 1383-7
[33] Bowden N, Brittain S, Evans A G, Hutchinson J W and Whitesides G M 1998 Spontaneous formation of ordered structures in thin films of metals supported on an elastomeric polymer *Nature* **393** 146-9
[34] Choi W M, Song J, Khang D-Y, Jiang H, Huang Y Y and Rogers J A 2007 Biaxially Stretchable "Wavy" Silicon Nanomembranes *Nano Letters* **7** 1655-63
[35] Timoshenko S P and Gere J M 1961 *Theory of elastic stability*: Courier Dover Publications
[36] 3M, VHB Adhesive Transfer Tapes with Adhesive 100MP: F9460PC, F9469PC, F9473PC, http://www.3m.com/, April 2005
[37] 3M, VHB Tapes: Technical Data, http://www.3m.com/, April 2014
[38] Lau, G. K., Goh, S. C. K., Shiau, L. L. 2011 Dielectric elastomer unimorph using flexible electrodes of electrolessly deposited (ELD) silver. Sensors and Actuators A: Physical, 169(1), 234-241.
[39] Low S H, Shiau L L and Lau G K 2012 Large actuation and high dielectric strength in metallized dielectric elastomer actuators *Applied Physics Letters* **100** 182901
[40] Efimenko K, Rackaitis M, Manias E, Vaziri A, Mahadevan L and Genzer J 2005 Nested self-similar wrinkling patterns in skins *Nat Mater* **4** 293-7
[41] Brochu P, Li H, Niu X and Pei Q 2010 Factors influencing the performance of dielectric elastomer energy harvesters. pp 76422J-J-12

Appendix A. Derivation of buckling force per unit length

A.1. Uniaxial buckling

For a uniaxially buckled thin film (see figure 2b), the out-of-plane deflections can be described by

$$w = \zeta \sin(\frac{\pi x}{l})$$

where ζ is the amplitude and l is the half-wavelength.

By assuming small deflections, the strain energy U in the thin film is equal to the bending energy

$$U = 0.5D \int_0^l \int_0^l \left(\frac{\partial^2 w}{\partial x^2}\right)^2 dxdy = \frac{lb}{4} D\zeta^2 \frac{\pi^2}{l^2}$$

The work done T by the axial force per unit length N_x to buckle the thin film is given by

$$T = 0.5 \int_0^b \int_0^l N_x \left(\frac{\partial w}{\partial x}\right)^2 dxdy = \frac{lb}{4} N_x \zeta^2 \frac{\pi^2}{l^2}$$

By using the principle of virtual work, wherein

$$\frac{\partial U}{\partial \zeta} \delta\zeta = \frac{\partial T}{\partial \zeta} \delta\zeta$$

The force per unit length N_x required to buckle the thin film is given by

$$N_x = D \frac{\pi^2}{l^2}$$

A.2. Biaxial buckling

For a biaxially buckled thin film (see figure 2c), the out-of-plane deflections can be described by

$$w = \zeta \sin(\frac{\pi x}{l}) \sin(\frac{\pi y}{b})$$

where ζ is the amplitude and l and b are the half-wavelengths in the x and y directions, respectively.

By assuming small deflections, the strain energy U in the thin film is equal to the bending energy

$$U = 0.5D\int_0^b\int_0^l\left(\frac{\partial^2 w}{\partial x^2}+\frac{\partial^2 w}{\partial y^2}\right)^2 dxdy = \frac{lb}{8}D\zeta^2\left(\frac{\pi^2}{l^2}+\frac{\pi^2}{b^2}\right)^2$$

The work done T by the axial forces per unit length N_x and N_y to buckle the thin film is given by

$$T = 0.5\int_0^b\int_0^l N_x\left(\frac{\partial w}{\partial x}\right)^2 + N_y\left(\frac{\partial w}{\partial y}\right)^2 dxdy = \frac{lb}{8}\zeta^2\left(N_x\frac{\pi^2}{l^2}+N_y\frac{\pi^2}{b^2}\right)$$

By using the principle of virtual work, wherein

$$\frac{\partial U}{\partial \zeta}\delta\zeta = \frac{\partial T}{\partial \zeta}\delta\zeta$$

and by assuming that $N_x = N_y$, the force per unit length required to buckle the thin film is given by

$$N_x = 4D\left(\frac{\pi^2}{l^2}+\frac{\pi^2}{b^2}\right)$$

By assuming a square plate wherein $b = l$,

$$N_x = 2D\left(\frac{\pi^2}{l^2}\right)$$

Appendix B. Radial stretcher.

A radial stretcher was custom-made to radially stretch and relax an elastomer membrane by moving the sixteen crocodile clips, which holds the circumference of the disc-like membrane. Equal radially outwards motions stretch the membrane, while equal radially inwards motions relax the membrane. Radial motions for the crocodile clips are controlled equally by a stepper motor, running at a rate of 3.6 D_0 per minute. To mitigate tearing, by the crocodile clips, the circumference of the elastomer membrane can be reinforced by a VHB layer of 5mm width. Once stretched to the required value, the stretched elastomeric membrane can be easily transferred to an annular-shape supporting frame. This can be done by fastening bolts and nuts, to secure each crocodile clip to the holes in the frame, and then unhooking the crocodile clips from the radial stretcher. The frame mounting enables easy handling of the stretched elastomer membrane for the deposition of metal thin films on both sides of the membrane. After that, in order to change the stretch in the elastomer membrane, it can be transferred back to the radial stretcher by re-hooking the crocodile clips to the stretcher and unfastening the bolts and nuts from the frame. In this way, the metalized dielectric elastomeric membrane can be relaxed from a higher to a lower stretch, in order to induce surface buckling that crumples the metal thin-film electrodes.

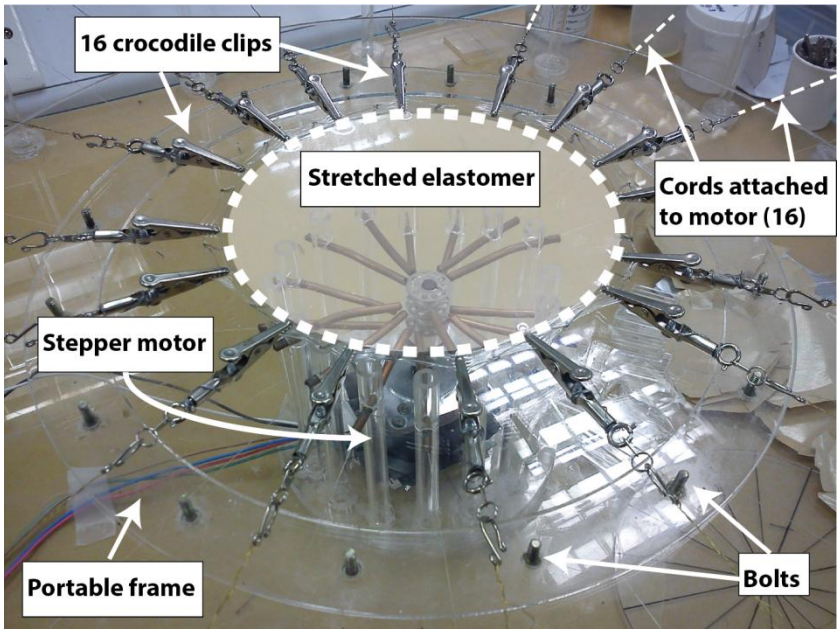

Figure B1. A radial stretcher used to fabricate the crumpled metal thin-film electrodes.

Appendix C. Cyclic loading of crumpled ELD silver electrodes

Crumpled ELD silver electrodes are able to sustain a cyclic uniaxial loading of between 0% and 100% strain. The crumpled ELD silver electrodes were 10mm by 10mm in size and had a compressive strain of 75% at zero apparent strain. The electrodes were cyclically strained, between 0% and 100% uniaxial strain, for one hundred times at a rate of 50% strain per minute. As shown in figure C1, the resistance of the crumpled silver thin-film electrodes remained low, below 60 Ω, throughout the one hundred cycles. After the first cycle, the resistance of the unstrained electrode, at 0% strain, increased from 33 Ω to 45 Ω. Thereafter, the unstrained electrode resistance decreased through the first 30 cycles and increased slightly through cycles 30 to 40. After the first 40 cycles, the electrode resistance stabilized; the unstrained electrode resistance was maintained at 42 ± 0.2 Ω while the 100%-strained electrode resistance was kept at 52 ± 0.2 Ω.

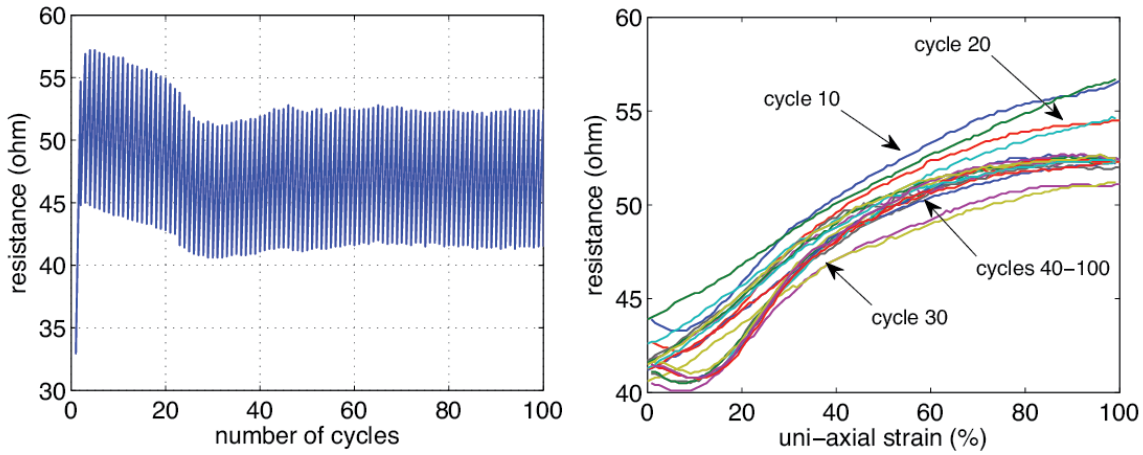

Figure C1. Change in resistance across the electrode as the crumpled ELD silver electrode was cyclically strained between 0% and 100% for a hundred times.